

# P-102: Amorphous Silicon Thin-Film Transistors-based Active-Matrix Organic Light-Emitting Displays

Joo-Han Kim and Jerzy Kanicki

Solid-State Electronics Laboratory, Dept. of EECS, The University of Michigan, Ann Arbor, MI, USA

## Abstract

In this paper, we describe hydrogenated amorphous silicon (a-Si:H) thin-film transistor (TFT)-based active-matrix arrays for active-matrix organic light-emitting displays (AM-OLEDs). The proposed pixel electrode circuits based on three a-Si:H TFTs can supply a continuous output current for AM-OLEDs. Each pixel circuit has compensation circuits that can adjust for the OLED and a-Si:H TFTs electrical characteristics shifts.

## 1. Introduction

In the past several years different types of the pixel electrode circuits have been proposed for the active-matrix (AM) organic light-emitting displays (OLEDs). For the micro-displays, crystalline silicon (c-Si) CMOS based pixel electrode circuits have been developed [1-3]. These AM-OLEDs have limited size (< 2 inch) and use organic light-emitting devices with the top transparent cathode electrode. For large - area AM-OLED, the polycrystalline silicon (poly-Si) thin film transistor (TFT) pixel electrode circuits have been introduced [4-7]. The advantage of poly-Si TFT AM-OLEDs is that the display drivers can be integrated with the pixel electrode circuits.

Another possible low cost technology for large area AM-OLED is hydrogenated amorphous silicon (a-Si:H) TFT technology. In our laboratory, we have developed a-Si:H TFT based AM-OLED for two driving schemes, current driven 4-a-Si:H TFT [8] and voltage driven 3-a-Si:H TFT pixel electrode circuits [9]. With the 4-TFT configuration, the perfect device parameter shift compensation and the resolution up to 200 dpi were achieved. A higher resolution AM-OLED can only be obtained with top ITO structure OLEDs.

We have also shown that AM-OLED having resolution up to 500 dpi, good device parameter shift compensation, simple active-matrix circuit construction, and the compatibility with the existing AM-LCD driving chips can be achieved with the 3-TFT pixel electrode configuration [10].

In this paper we describe the design, fabrication and electrical properties of the active-matrix arrays based on 3-a-Si:H TFT pixel electrode circuits that we used for the active-matrix organic light-emitting displays.

## 2. 3-a-Si:H TFTs Pixel Electrode Circuits

### 2.1 Pixel Operation

In AM-OLED, in order to turn on OLED continuously, a minimum of two TFTs are needed. It should be noticed that, in this type of pixel electrode circuits, any variation of TFTs or OLEDs electrical parameters (threshold and turn-on voltages) will introduce different output current levels for each pixel even if the driving TFT gate-source voltage and drain-source voltage are kept constant. This output current non-uniformity will result in OLED brightness non-uniformity since OLED luminance is usually proportional to applied current level. To overcome this problem, a

voltage driven 3 - a-Si:H TFT pixel design was developed in our laboratory.

The 3 - a-Si:H TFT pixel electrode circuit and the voltage driving scheme are shown in Figure 1 [10]. Each pixel circuit features 3 TFTs. In this schematic diagram,  $C_{ST}$  is storage capacitor, T1 is switching TFT, T2 is active resistor, and T3 is large-sized high-capacity constant current driving TFT. Switching transistor is used to select the pixel while  $V_{select}$  is on. The image data are 0 to 15 V voltage signals ( $V_{data}$ ) in this example.

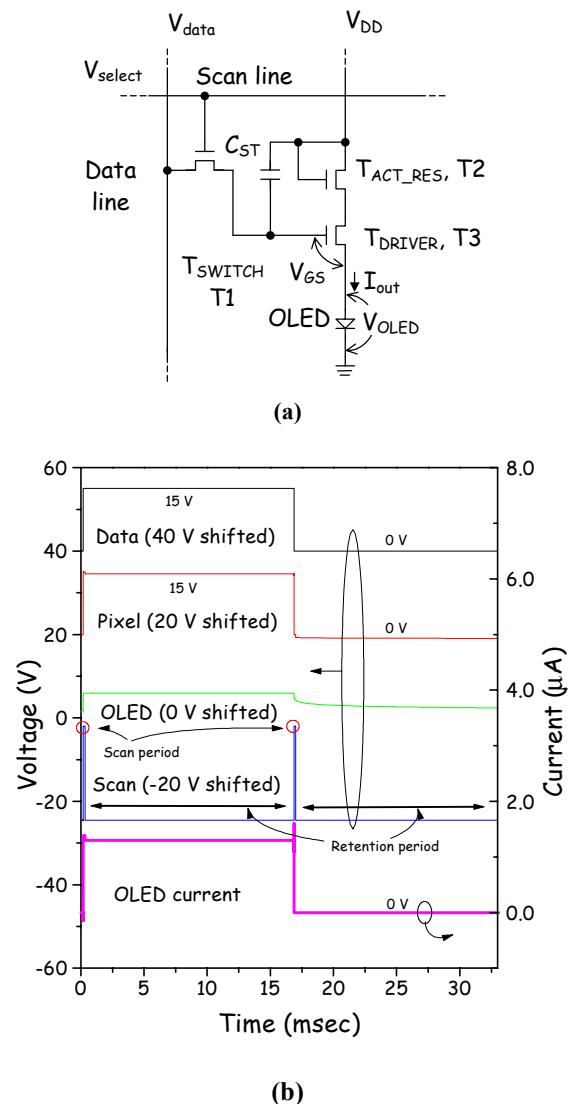


Figure 1. A (a) schematic diagram of the AM-OLED pixel electrode circuit [10] and a (b) simulation example of the AM-OLED operation for data voltages of 15 V.

During the scan time, the data voltage,  $V_{data}$ , is stored in the storage capacitor. The driver TFT provides the corresponding current (driving current) to the OLED. For a given frame time depending on the refresh rate of the AM-OLED design, the gate voltage of the constant current driving TFT remains at the same level even after  $V_{scan}$  drops low, since  $C_{ST}$  keeps the image data ( $V_{data}$ ) during the retention period.

The current compensation circuit is represented by an active resistor (T2) TFT operating only in saturation mode. The drain electrode of the driving TFT is connected to a high-voltage source ( $V_{DD}$ ) through the active resistor. The operating current ( $I_{out}$ ) determines the voltage drop across the active resistor. Any unstable current level shift during the display operation will be compensated by the active resistor. For any reason, e.g., when the TFT threshold voltage of the constant current driver or the OLED turn-on voltage increases, if the current flowing through the active resistor decreases, the voltage drop across the active resistor decreases. That will allow for a high current to flow back through the OLED pixel, compensating for the device parameter changes in both the constant current driver TFT and the OLED.

### 2.2 Pixel Electrode Design and Fabrication

The pixel electrode circuit performance of our AM-OLED was simulated using the circuit simulator, HSPICE. Using the OLED and a-Si:H TFT models developed during this research, an active-matrix array of 640 x 480 pixels (VGA) for AM-OLED with 200 dpi resolution (127  $\mu\text{m}$  x 127  $\mu\text{m}$  pixel size) was designed and simulated for data voltages ( $V_{data}$ ) ranging from 0 to 15 V. An example of the transient pixel electrode circuits simulation is shown in Figure 1 (b), where we plot two image data voltages of 15 and 0 V for maximum and minimum output current cases, respectively. The operation condition of our pixel electrode circuit was visualized using the load line technique as show in the Figure 2. The proper sizing of each TFTs (W/L) was determined through the circuit simulation.

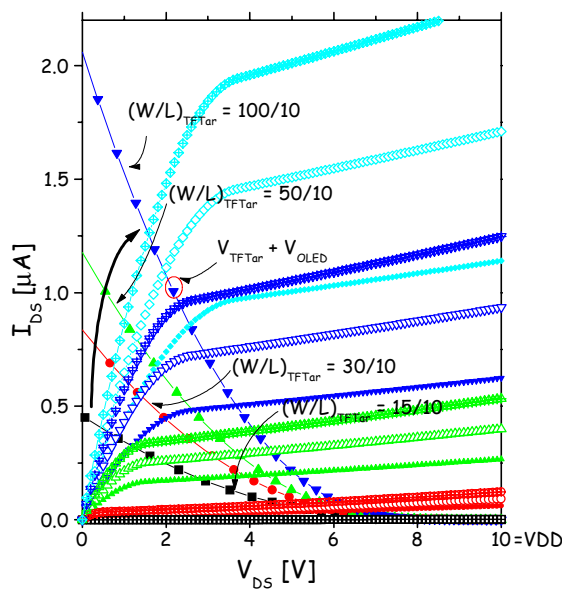
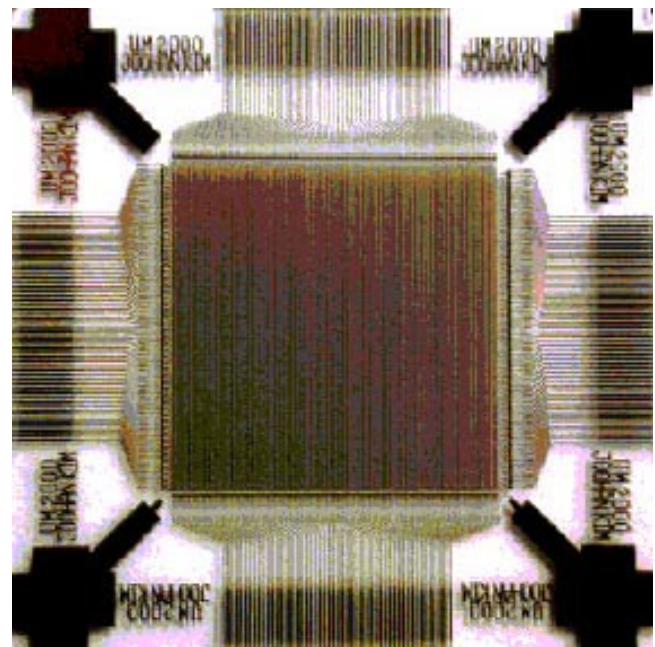
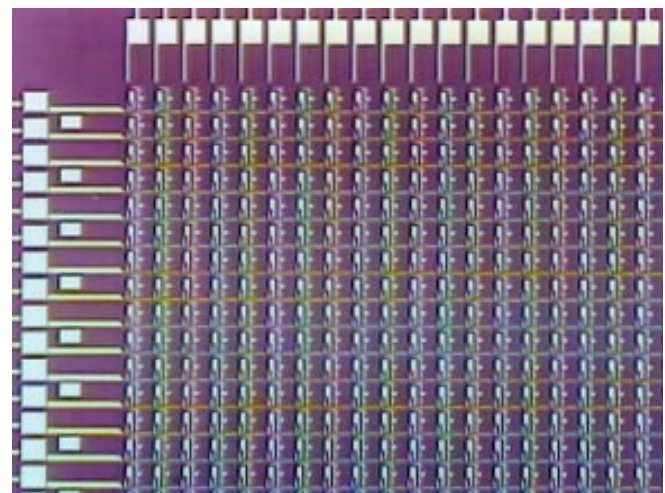


Figure 2. Load line for optimizing TFT sizes.

Based on our design, 3 – a-Si:H TFT AM-OLED has been successfully fabricated. Figure 3 shows the top views of the quarter-size active-matrix arrays and the AM-OLED panel. A continuous pixel electrode excitation was achieved with these circuits, and the output driving current level was reached up to 1.3  $\mu\text{A}$  with this a-Si:H TFT technology. The conventional back-channel etched (BCE) TFTs technologies were used with  $n^+$  a-Si:H/a-Si:H/a-SiN<sub>x</sub>:H layers deposited by PECVD technique at substrate temperature of 300 °C. All PECVD films used in this work were deposited at Philips Research Laboratory, United Kingdom. The processing of active-matrix arrays was accomplished at the Solid-State Electronics Laboratory of The University of Michigan.



(a)



(b)

Figure 3. Top view of the AM-OLED designed and fabricated in our laboratory.

In the present case, 100 x 100 lines AM-OLED with 200 dpi resolution was fabricated as engineering demonstrator. The storage capacitance was also optimized during the AM-OLED simulation. The optimum value was chosen to be large enough for good image retention and to fit into the pixel area. In our case, the storage capacitor is 0.4 pF, and the pixel aperture ratio is 45 % for this pixel design. With a storage capacitance of 0.4 pF, the switching between the ON- and OFF-states was completed within the scan time. In addition, the image data stored in the storage capacitor was retained without any loss during the retention period for AM-OLED frame time (60 Hz). In the present design, OLED area is 7200  $\mu\text{m}^2$ .

The electrical characteristics of the individual TFTs used in this AM-OLED are shown in Figure 4. From the  $I_D$ - $V_D$  characteristics, Figure 4 (a) inset, the drain current of the Driver TFT is well saturated. The ON-current was about 10  $\mu\text{A}$  for the data voltage of 10 V. The current level is well modulated for different data voltages in the  $I_D$ - $V_G$  curves, Figure 4 (a).

The switching transistor shows similar behavior in terms of both  $I_D$ - $V_D$  and  $I_D$ - $V_G$  characteristics. The ON-current was high enough to transfer the data voltage to the storage capacitor with a video rate display performance, Figure 4 (b). The active resistor shows its saturation mode operation, Figure 4 (c). When there is small drop in the drain current level, the corresponding voltage drop is fed back to the driver TFT in order to stabilize the driving current level.

For driver and switching TFTs, the ON-current ranged from 1 to 20  $\mu\text{A}$  with W/L ranging from 1 to 10. The linear field-effect mobility,  $\mu_{FE}$  was around 0.2  $\text{cm}^2 / \text{Vsec}$  with the threshold voltage of 0.6 V for both TFTs. We observed a small current crowding at small  $V_{DS}$  (Figures 4 (a) & (b) insets) and high OFF-current at large  $V_{DS}$  (Figure 4 (a) & (b)). This was due to thick a-Si:H layer and un-optimized active-matrix process conditions.

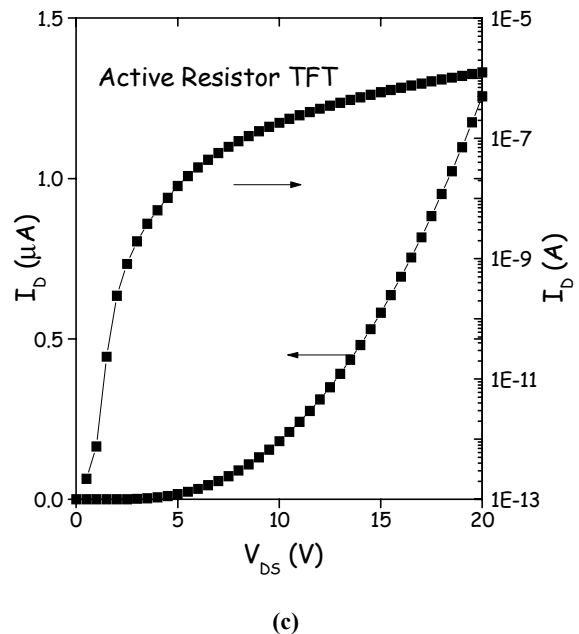
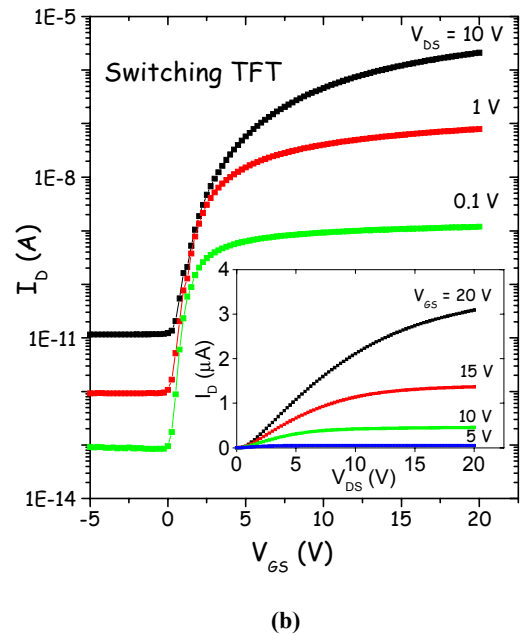
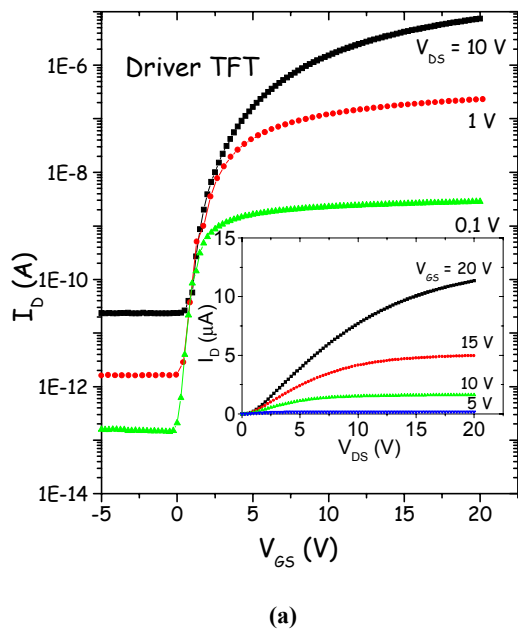


Figure 4. The electrical characteristics for (a) driver, (b) switching, and (c) active resistor a-Si:H TFTs.

The output current of our AM-OLED pixel was measured with  $V_{DD} = 20 \text{ V}$  and  $V_{scan} = 20 \text{ V}$ , Figure 5. The maximum current density of 21  $\text{mA} / \text{cm}^2$  was achieved for the aperture ratio of 45 % in our design. However, the current density level can be adjusted from 5 to 100  $\text{mA} / \text{cm}^2$  by increasing the driver TFT dimension with a loss of the pixel aperture ratio.

For  $I_{out} = 100 \text{ mA} / \text{cm}^2$ , the pixel aperture ratio would be around 25 % according to our calculation having resolution from 200 to 500 dpi. The deviation between the simulated and measured

results is mainly due to un-optimized active-matrix fabrication process conditions as mentioned above.

The corresponding OLED brightness for the output current level of 21  $\mu\text{A} / \text{cm}^2$  are 4500, 210, and 190  $\text{cd} / \text{m}^2$  for green (540 nm), blue (480 nm), and red (650 nm). In this case, OLED external quantum efficiency is assumed to be 5, 1.5, and 2 %, respectively, Figure 6.

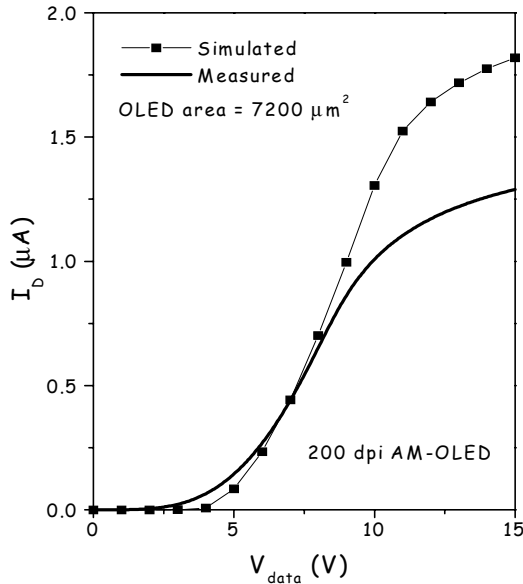


Figure 5. The measured AM-OLED output current versus input data voltage characteristics.

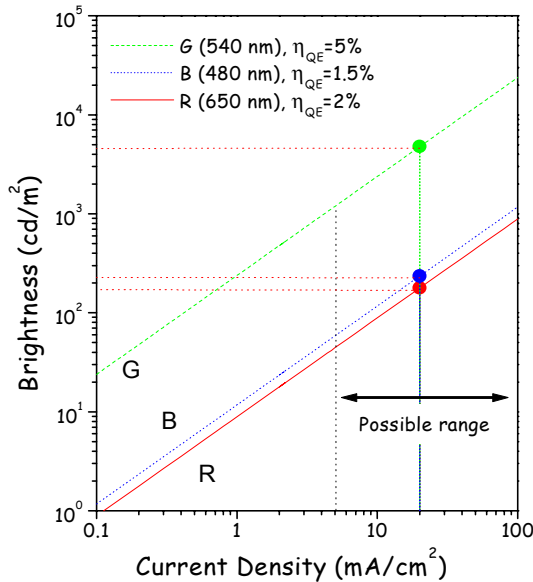


Figure 6. The maximum OLED brightness of each pixel for RGB color scales.

The maximum OLED brightness level possible with our pixel electrode circuits are 24000, 1200, and 900  $\text{cd} / \text{m}^2$  for green, blue, and red respectively in the case  $I_{\text{out}} = 100 \mu\text{A} / \text{cm}^2$ . The luminance shown in Figure 6 was calculated as follows:

$$L = 683 \times E(\omega) \cdot \eta_{\text{ex}} \cdot \frac{hc}{\pi\omega} \cdot \frac{J}{e}$$

where E is the normalized luminous efficiency (0.107, 0.954, and 0.139 for red, green, and blue, respectively, from photopic eye response curve),  $\omega$  is the wave length,  $\eta_{\text{ex}}$  is the device external quantum efficiency, h is the Planck constant, c is the velocity of light, e is the electronic charge, and J is the applied current density. The OLED brightness levels for different colors will increase with the increase of the external quantum efficiencies.

### 3. Conclusion

We have demonstrated that it is possible to develop a high-resolution and large-area AM-OLED based on a-Si:H TFT technology. The pixel electrode circuits simulation and experimental results indicate that a continuous pixel electrode excitation can be achieved with these pixel circuits, and a pixel electrode driving output current level up to 1.3  $\mu\text{A}$  was reached with the a-Si:H TFT technology in the present study. The output current density level can be increased up to 100  $\mu\text{A} / \text{cm}^2$  for optimized pixel electrode circuits.

### 4. Acknowledgements

We thank NIH for the financial support of this project. The PECVD films used in this work were provided by Dr. Ian French (Philips Research Laboratory, U.K.).

### 5. References

- [1] K. Pichler et al., *Proc. of SPIE*, 3797, 258 (1999).
- [2] T. Feng et al., *Proc. of SPIE*, 4105, 30 (2001).
- [3] H.E. Abraham et al., *Proc. of SPIE*, 4105, 37 (2001).
- [4] R.M.A. Dawson et al., *Proc. of SID Sym.*, p. 11 (1998).
- [5] M. Kimura et al., *IEEE Trans. on Elec. Dev.*, 46, 2282 (1999).
- [6] T. Shimoda et al., *Proc. of IEDM*, p. 107 (1999).
- [7] M. Mizukami et al., *Proc. of SID Sym.*, p. 912 (2000).
- [8] Yi He et al., *IEEE EDL*, 21, 590 (2000).
- [9] J. Kanicki et al., *Proc. IDRC* (2001).
- [10] J.-H. Kim et al., *Proc. SPIE Medical Imaging*, 4319, 306 (2001).